NASA TECHNICAL NOTE

NASA TN D-8501

CHEMICAL KINETIC MODELING OF PROPANE OXIDATION BEHIND SHOCK WAVES

Allen G. McLain and Casimir J. Jachimowski

Langley Research Center
Hampton, Va. 23665

NATIONAL AERONAUTICS AND SPACE ADMINISTRATION • WASHINGTON, D. C. • JULY 1977

1. Report No. NASA TN D-8501	2. Government Accession No.	3. Recipient's Catalog No.
4. Title and Subtitle CHEMICAL KINETIC MODELING OF PROPANE OXIDATION BEHIND SHOCK WAVES		5. Report Date July 1977 6. Performing Organization Code
7. Author(s) Allen G. McLain and Casimir J. Jachimowski		8. Performing Organization Report No. L-11606
9. Performing Organization Name and Address NASA Langley Research Center Hampton, VA 23665		10. Work Unit No. 505-03-31-01 11. Contract or Grant No.
12. Sponsoring Agency Name and Address National Aeronautics and Space Administration Washington, DC 20546		13. Type of Report and Period Covered Technical Note 14. Sponsoring Agency Code

15. Supplementary Notes

16. Abstract

The stoichiometric combustion of propane behind incident shock waves was studied experimentally and analytically over a temperature range from 1700 K to 2600 K and a pressure range from 1.2 to 1.9 atm. Measurements of the concentrations of carbon monoxide [CO] and carbon dioxide [CO_2] and the product of the oxygen atom and carbon dioxide concentrations [O][CO] were made after passage of the incident shock wave. A kinetic mechanism was developed which when used in a computer program for a flowing, reacting gas behind an incident shock wave predicted experimentally measured results ([CO], [CO_2], [O][CO], and reaction times) quite well. Ignition delay times from the literature were also predicted quite well. The kinetic mechanism consisted of 59 individual kinetic steps.

17. Key Words (Suggested by Author(s)) Kinetics Reaction mechanisms Shock waves	18. Distribution Statement Unclassified - Unlimited Subject Category 25		
19. Security Classif. (of this report) Unclassified	20. Security Classif. (of this page) Unclassified	21. No. of Pages 30	22. Price* $4.00

* For sale by the National Technical Information Service, Springfield, Virginia 22161

CHEMICAL KINETIC MODELING OF PROPANE OXIDATION BEHIND SHOCK WAVES

Allen G. McLain and Casimir J. Jachimowski
Langley Research Center

SUMMARY

The stoichiometric combustion of propane behind incident shock waves was studied experimentally and analytically over a temperature range from 1700 K to 2600 K and a pressure range from 1.2 to 1.9 atm. Measurements of the concentrations of carbon monoxide [CO] and carbon dioxide [CO_2] and the product of the oxygen atom and carbon dioxide concentrations [O][CO] were made after passage of the incident shock wave. A kinetic mechanism was developed which when used in a computer program for a flowing, reacting gas behind an incident shock wave predicted experimentally measured results ([CO], [CO_2], [O][CO], and reaction times) quite well. Ignition delay times from the literature were also predicted quite well. The kinetic mechanism consisted of 59 individual kinetic steps.

INTRODUCTION

The ability to model successfully the kinetics of hydrocarbon oxidation, particularly for high-molecular-weight hydrocarbons, is important in the development of reliable mathematical models of combustion systems, such as aircraft gas turbine combustors. Even though much work has been done in the area of combustion chemistry, very few experimentally validated chemical kinetic models are available. However, as a result of such work, guidelines for the assembly of hydrocarbon combustion models do exist.

Recent experimental studies of the oxidation of high-molecular-weight hydrocarbons have indicated that these long-chain molecules decompose rapidly during early stages of combustion into hydrocarbon molecules and fragments with lower molecular weights. For instance, reference 1 indicated that larger hydrocarbons (iso-octane and n-heptane) degraded rapidly into ethylene, carbonyls, C_3 olefins, and acetylene. Interestingly, this rapid decomposition was also noted in a study (ref. 2) of the oxidation of ethane, the next hydrocarbon above methane in the alkane series. After scrutiny of hydrocarbon combustion literature, Cooke and Williams suggested in reference 3 that rapid decomposition of the parent fuel followed by oxidation of the low-molecular-weight hydrocarbon molecules and fragments best described mechanistically the combustion behavior of long-chain alkane hydrocarbons. Because of these observations, a kinetic rate mechanism which can explain the combustion behavior of a high-molecular-weight alkane (propane, for instance) must incorporate kinetic steps observed for simpler hydrocarbons (CH_4, C_2H_2, C_2H_4, and C_3H_6). In reference 4, methane oxidation behind shock waves was studied and a kinetic rate mechanism was developed which, when used in an analytical model for a flowing, reacting gas behind a shock wave, gave results that agreed well with experimental data. In a subsequent study (ref. 5), both acetylene and ethylene oxidation behind shock waves was studied over the temperature range from 1700 to 2600 K, and a kinetic rate

mechanism was developed. This rate mechanism, incorporating kinetic steps from methane combustion, gave analytical results which again compared well with experimental data. The logical extension of this work is the study of the combustion of propane and the development and verification of a kinetic rate mechanism in which the propane decomposition reactions are coupled with the reactions that described oxidation of fragments with lower molecular weights, such as the methyl radical, acetylene, and ethylene.

The decomposition and ignition characteristics of propane have been studied extensively in references 6 to 10. In reference 11, Chinitz and Baurer presented a lengthy kinetic rate mechanism for propane in which many of the rate constants were calculated from the kinetic theory of gases and empirical relations for estimating the Arrhenius preexponential factor and the activation energies. A number of the elementary reactions in this mechanism appear in the methane, acetylene, and ethylene kinetic mechanisms mentioned previously. However, this lengthy mechanism assumed the formation of a number of oxygenated intermediates (not observed experimentally) and also relied on radical reactions as the primary path for destruction of the propane.

The purpose of this paper is to present the results of the stoichiometric oxidation of propane behind shock waves at temperatures between 1700 K to 2600 K and pressures between 1.2 to 1.9 atm. The progress of the oxidation reactions behind the shock waves was monitored by measuring the emitted radiation from carbon monoxide, carbon dioxide, and the chemiluminescent reaction, $O + CO \rightarrow CO_2 + h\nu$. The measured intensity of the radiation was used to calculate concentrations of carbon monoxide and carbon dioxide and the product of the oxygen atom and carbon monoxide concentrations. A kinetic rate mechanism was assembled, and with the use of the analytical model of reference 12 for a flowing, reacting gas behind incident shock waves, a parametric study of the kinetic mechanism was made. Predicted and measured concentrations and reaction times were compared during the study resulting in the evolution of a kinetic mechanism for propane. Ignition delay times were predicted by the developed kinetic mechanism and were compared with experimental ignition delay times from reference 6.

SYMBOLS

$[CO]$, $[CO_2]$	molar concentrations of CO and CO_2, mol/cm^3
$[O][CO]$	concentration product of atomic oxygen and carbon monoxide, $(mol/cm^3)^2$
E_λ	voltage measured with specific detectors and filters of wavelength λ, V
$h\nu$	radiation emitted during chemiluminescent reaction, $O + CO \rightarrow CO_2 + h\nu$
k	rate coefficient, sec^{-1} for unimolecular reactions, $cm^3/mol\text{-}sec$ for bimolecular reactions, $cm^6/mol^2\text{-}sec$ for termolecular reactions
p	pressure, atm (1 atm = 101.3 kPa)
T	absolute temperature, K

T_m temperature predicted by kinetic model, K

t_i ignition delay time, μsec

t_m reaction time, μsec

Abbreviations:

IR infrared

UV ultraviolet

EXPERIMENTAL APPARATUS AND MEASUREMENTS

All experiments were carried out behind incident shock waves in a stainless-steel shock tube with an inside diameter of 8.9 cm. Approximately half of the tests were carried out in a 580-cm-long test section with an observation station located 565 cm from the diaphragm location (station ① in fig. 1), and the other half were carried out in a 671-cm-long test section with an observation station located 625 cm from the diaphragm location (station ② in fig. 1). This test section and observation stations were used in the studies of references 4 and 5.

Figures 2(a) and (b) are graphical illustrations of the 565-cm and 625-cm observation stations, respectively. Infrared monitoring equipment at the 625-cm observation station (fig. 2(b)) consisted of two indium antimonide infrared detectors mounted on opposite sides of the shock tube. At 90° from this location, a photomultiplier and a pressure or heat-transfer gage were mounted on opposite sides of the shock tube. The infrared detectors and the photomultiplier were rigidly mounted to the shock tube with an adapter which contained a calcium fluoride window, collimating slits, and an interference filter of the appropriate wavelength for observing emission from CO, CO_2, or the chemiluminescent reaction, $O + CO \rightarrow CO_2 + h\nu$. The interference filter used to monitor CO_2 radiation was centered at 4.3 μm with a bandwidth at half-peak of 0.15 μm, while an interference filter centered at 5.0 μm with a bandwidth at half-peak of 0.15 μm was used to monitor radiation from CO. The interference filter used with the photomultiplier (having an S-20 response) for monitoring the radiation from the reaction, $O + CO \rightarrow CO_2 + h\nu$, was centered at 3700 Å with a bandwidth at half-peak of 65 Å. The fourth location at this observation station was equipped with either a dynamic pressure gage or a heat-transfer gage which could be used to trigger counters or to indicate shock arrival at the observation station.

In the 580-cm-long test section (fig. 2(a)), only two measurements (emission from the reaction, $O + CO \rightarrow CO_2 + h\nu$, and emission from either CO or CO_2) could be made behind the incident shock wave for each run. Thus, two runs were required to collect $[O]$ $[CO]$, $[CO]$, and $[CO_2]$ data. In addition, a monochromator was used to collect the radiation at 3700 Å for the chemiluminescent reaction, $O + CO \rightarrow CO_2 + h\nu$. The monochromator was equipped with a grating blazed at 3000 Å and a photomultiplier with an S-20 response. The slits were set to allow

a half-peak bandwidth of 32 Å at the 3700-Å setting. The windows were calcium fluoride, and a quartz lens with a focal length of 80 mm was used to pick up the radiation from the center of the tube and focus it on the entrance slit of the monochromator. Slits placed between the calcium fluoride windows and the monochromator reduced the field of view to provide less than 2 μsec of time resolution in flowing gas. The infrared equipment used to monitor the emission from CO and CO_2 was the same as for the 625-cm observation station.

The following calibration procedure was used at both the 565-cm and 625-cm observation stations. The infrared detection system was calibrated by shock heating a mixture of CO or CO_2 diluted with argon and recording the intensity of the emitted radiation as a voltage output on an oscilloscope. A quantitative relationship was established between the intensity of the radiation measured from the CO or CO_2 and the concentration of CO or CO_2 in the test section over a range of temperature from 1700 K to 2600 K.

The voltage output and the calibration curves for the CO_2 and CO infrared detectors are presented in figures 3 and 4, respectively. Figures 3(a) and 4(a) illustrate the variation in voltage output from the infrared detectors equipped with the 4.3-μm and 5.0-μm filters for different mole fractions of CO_2 or CO in the test gas mixtures. Figures 3(b) and 4(b) illustrate the empirical quantitative relationships developed between $[CO_2]$ and [CO] and the measured voltages and temperatures. Since the CO_2 emission band overlaps the CO emission at 5.0 μm, a correction was necessary to obtain the true CO concentrations. To make this correction, a correlation between the temperature and the ratio of the voltages measured at 5.0 μm and 4.3 μm was determined for various CO_2-Ar mixtures. This correlation is shown in figure 5.

For the reaction, $O + CO \rightarrow CO_2 + h\nu$, the detection system was calibrated by shock heating a mixture of H_2-O_2-CO-CO_2-Ar over the same temperature range and recording the chemiluminescent emission. Details of this calibration procedure are given in references 4 and 5.

The output voltage with respect to time was displayed on an oscilloscope and photographed. The time constant for the infrared recording system was about 3 μsec. For the ultraviolet recording system, the time constant was less than 2 μsec. The speed of the shock wave was measured with a raster system upon which timing marks were superimposed at 10- or 50-μsec intervals. On this same raster, output voltage deflections from heat-transfer gages located 30.48 cm apart indicated shock passage. In addition, the heat-transfer gage output at station ① was used to start a counter operating in tenths of microseconds. The heat-transfer gage or dynamic pressure transducer at observation station ② yielded a voltage output which was used to stop the counter. The time for the shock wave to pass from station ① to the observation station ② was used to calculate the shock velocity at the instant of arrival of the shock wave at the observation location. The times from the raster and the counter compared well.

The test gas mixture was prepared by the method of partial pressures from commercially prepared propane (99.5 percent), oxygen (99.7 percent), and argon (99.995 percent) without further purification. Samples of the mixture were analyzed with a commercially available hydrocarbon analyzer for the percentage of propane in the mixture which was found to vary not more than $\pm$0.1 percent from

the desired value. The initial test gas pressure was 40 torr (1 torr = 133.3 Pa) for all tests.

EXPERIMENTAL RESULTS AND DATA ANALYSIS

An example of the experimental data obtained by shock heating a mixture (1-percent C_3H_8, 5-percent O_2, and 94-percent Ar by volume) is shown in figure 6. The traces represent the oscilloscopic display of voltage output of the $[CO][O]$, $[CO]$, and $[CO_2]$ optical detection equipment as changes occurred with time. These traces are typical of the mixture being studied. All the $[CO][O]$ chemiluminescent ultraviolet emission profiles at 3700 Å exhibited a pronounced spike a short time after shock arrival followed by a slow decrease. Similar features were observed in references 4 and 5 during the combustion of methane, acetylene, and ethylene behind shock waves. The infrared emission profiles for CO_2 at 4.3 μm and CO at 5.0 μm always exhibited a rapid increase after shock arrival followed by a knee and then a region of very slow increase. The knee of each infrared emission profile occurred slightly after the 3700-Å emission spike.

The 3700-Å emission profile was analyzed by the method outlined in reference 4. The entire postspike emission was assumed to be from the chemiluminescent reaction, $O + CO \rightarrow CO_2 + h\nu$. The maximum in this reaction's emission was assumed to occur at the same time as the maximum for the emission spike. By extrapolation of the postspike emission into the spike region, a maximum for the $O + CO \rightarrow CO_2 + h\nu$ reaction profile was obtained. The voltage at this maximum was used to calculate the concentration product $[O][CO]$. The $[O][CO]$ values calculated by this method and the reaction times t_m defined as the interval (laboratory time) between shock arrival and the emission maximum are presented in table I. The uncertainty in calculating the $[O][CO]$ product in this manner was estimated to be 5 to 10 percent from the analysis in reference 4. The temperatures T in table I correspond to the temperatures immediately behind the shock before any reactions in the system could occur. These temperatures were calculated from the computer program of reference 12 given the experimentally obtained shock velocity and assuming frozen shock conditions. Although the temperature at the time of the maximum in the $[O][CO]$ profile is greater than at the shock front, a temperature correction was not deemed necessary since the difference in temperature would reduce the $[O][CO]$ product by less than 3 percent which is within the experimental scatter of the data.

For reduction of the infrared data, however, the temperature at the maximum of the $[O][CO]$ profile must be used. The $[CO]$ and $[CO_2]$ concentrations varied by as much as 20 percent and 60 percent, respectively, with temperature differences as large as those between the frozen shock temperature and the temperature at the $[O][CO]$ maximum ($\approx$200 K). For this reason, the temperature predicted by the kinetic model, T_m in table I, was used to calculate $[CO]$ and $[CO_2]$. The justification for the use of T_m is discussed in detail in reference 5.

COMPARISON BETWEEN EXPERIMENTAL RESULTS AND KINETIC MODELS

Propane decomposition and oxidation behind shock waves have been investigated in previous shock-tube experiments (refs. 6 to 8). One of these investigations (ref. 6) concentrated on the ignition characteristics of propane. Another (ref. 8) concentrated on the decomposition of propane behind a reflected shock wave and suggested a sequence of reaction steps and rate constants which analytically predicted the experimental measurements of the investigation. Using this information, a reaction scheme was assembled which could be studied parametrically to determine the influence of individual steps in achieving a good comparison with the experimental measurements of this paper as well as with ignition delay time data from reference 6. The preliminary kinetic mechanism with the associated rate coefficients is listed in table II. The rate coefficients were obtained from the literature whenever possible. (See refs. 4, 5, 8, 13, 14, and 15.) The rate coefficient for reaction (1) was estimated by using the value reported by Lifshitz and Frenklach (ref. 8) at 1200 K and assuming an activation energy equal to the bond dissociation energy. The rate coefficients for reactions (6) and (7) were estimated using Semenov's rule (ref. 16) to determine the activation energy and the Arrhenius factor was arbitrarily set at 5.00×10^{13} $cm^3/mol\text{-}sec$. For reaction (14), a zero activation energy was assumed since the reaction is highly exothermic, and the rate coefficient was set at 10^{13} $cm^3/mol\text{-}sec$.

The analytical model used in the parametric study involved one-dimensional flow behind an incident shock wave with finite-rate chemical reactions and boundary-layer growth. The basic computer program is described in reference 12; however, a modified form of this computer program described in reference 17 was used for most of the calculations because of its faster computational times for systems containing many species and reactions. The thermochemical data of JANAF (ref. 18) were used for the species involved in the mechanism; however, when JANAF data were not available, the data of reference 19 were used.

The parametric study was performed to obtain a good comparison between the present experimental results for the [O] [CO] product and the product calculated by the analytical model. Only the rate constants involving propane (reactions (1) to (14)) were manipulated within the suspected error limits. At the same time the additional restraint was imposed that the same rate mechanism must reproduce reasonably well the ignition delay time data presented in reference 6. The ignition delay time calculations were made with the same computer programs (refs. 12 and 17) operating in a manner which would simulate conditions behind a reflected shock wave, the condition under which the ignition delay time data of reference 6 were taken.

The first objective of the parametric study was to identify reactions which significantly influence the predicted [O] [CO] profiles, reaction times t_m, and ignition delay times t_i. To do this, the rate coefficients for reactions (1) and (14) were varied by a factor of 100, for reactions (2), (3), (10), (11), (12), and (13) by a factor of 10, and for reactions (4) to (9) by a factor of 4. The predicted [O] [CO] profiles, reaction times, and ignition delay times were found to be most sensitive to the rates of the following reactions:

(1) $C_3H_8 \rightarrow CH_3 + C_2H_5$

(2) $CH_3 + C_3H_8 \rightarrow CH_4 + n\text{-}C_3H_7$

(3) $CH_3 + C_3H_8 \rightarrow CH_4 + i\text{-}C_3H_7$

(10) $n\text{-}C_3H_7 \rightarrow C_2H_4 + CH_3$

(12) $n\text{-}C_3H_7 \rightarrow C_3H_6 + H$

(13) $i\text{-}C_3H_7 \rightarrow C_3H_6 + H$

The predicted [O] [CO] profiles and reaction times, however, were influenced most by the rate of reaction (1), whereas the predicted ignition delay times were influenced most by the rates of reactions (1), (2), and (3). The reaction mechanism and rate coefficients listed in table II predicted [O] [CO] values that were about 50 percent larger than the measured values and reaction times that were about a factor of 2 smaller. The predicted ignition delay times were from 10 to 50 percent smaller than the measured values.

In the final phase of the analytical study, an attempt was made to find a set of rate coefficients for the six reactions that would reproduce as well as possible the experimental data without resorting to unreasonable rate coefficients. Initially, the rate coefficient for reaction (1) was adjusted to provide reasonable agreement between the predicted and measured [O] [CO] values while the rate coefficients for reactions (2), (3), (10), (12), and (13) were fixed. It was found that best agreement was obtained when the decomposition of propane was written as a bimolecular process

(1) $M + C_3H_8 \rightarrow CH_3 + C_2H_5 + M$

with the rate coefficient, $k_1 = 5.00 \times 10^{15} \exp(-32\ 713/T)$ $cm^3/mol\text{-}sec$. The need to describe the decomposition of propane as a second-order process with an activation energy less than the bond dissociation energy suggests that the decomposition reaction is in the fall-off region of a unimolecular decomposition process. Similar behavior has been observed for methane (ref. 20) and methanol (ref. 21). The measured and predicted reaction times were also in good agreement.

After the rate coefficient for reaction (1) had been established, an attempt was made to find a set of rate coefficients for the other reactions that reproduced as well as possible the measured ignition times. With the adjusted rate coefficient for reaction (1), the predicted ignition times were substantially larger (a factor of 2 or greater) than the measured values. The ignition times could be decreased in four ways: by increasing the rates of reactions (2) and (3), by decreasing the rate of reaction (10), by increasing the rates of reactions (12) and (13), or by a combination of the above. Each of the four ways was attempted; however, a set of rate coefficients could not be found that were considered reasonable and that did not significantly influence the predicted [O] [CO] values and reaction times. Therefore, it appeared reasonable to reexamine the proposed reaction scheme to determine the cause of the long predicted ignition delay times. After examining several computer runs, it became

obvious that the long ignition delays were caused by reaction (15) which tied up the hydrogen radical, and since no removal reaction was present other than decomposition, there was a large buildup of the HO_2 radical. To remedy this, two reactions were added to the preliminary scheme (see table III):

(58) $H + HO_2 \rightarrow OH + OH$

(59) $CO + HO_2 \rightarrow OH + CO_2$

The rate coefficient for reaction (58) was set at (ref. 13)

$$2.5 \times 10^{14} \exp(-950/T) \text{ cm}^3/\text{mol-sec}$$

An experimental rate coefficient for reaction (59) could not be found; however, a recent study (ref. 22) of reaction (25), $CO + OH \rightarrow CO_2 + H$, suggested that the rate coefficient for reaction (59) must be significantly smaller than the rate coefficient for reaction (25). Therefore, the rate coefficient for reaction (59) was set at 10^{10} $\text{cm}^3/\text{mol-sec}$ which is about a factor of 10 smaller than the rate coefficient for reaction (25) over the temperature range of this study.

By incorporating these reactions into the reaction scheme, the predicted ignition delay times were substantially smaller, especially at lower temperatures but still about 50 percent higher than the measured values. The predicted $[O][CO]$ values and reaction times were not affected by these reactions. Better agreement between the measured and predicted ignition times was obtained by adjusting the rate coefficient of reactions (2) and (3) to

$$2.00 \times 10^{13} \exp(-5184/T) \text{ cm}^3/\text{mol-sec}$$

No attempt was made to vary the rate coefficients between reactions (2) and (3). This rate coefficient is about a factor of 5 larger than the value reported by Lifshitz and Frenklach (ref. 8) but is not an unreasonable rate coefficient for this type of reaction. A comparison of the predicted and measured $[O][CO]$ values is given in figure 7, and of the ignition delay times in table IV. Figure 8 shows the comparison between the predicted and measured concentrations of CO and CO_2 over the temperature range of this study. Figure 9 shows the comparison of predicted and measured reaction times t_m. In all the comparisons, the values predicted using the final kinetic mechanism agreed well with the experimental data.

The final kinetic mechanism for propane is listed in table III. The entire mechanism consists of 59 kinetic steps. To reduce the number of kinetic steps for the propane mechanism, it was found that the following reactions can be omitted from the mechanism without changing the computed values:

(36) $C_2H_4 + C_2H_4 \rightarrow C_2H_5 + C_2H_3$

(35) $C_2H_4 + M \rightarrow C_2H_3 + H$

(46) $C_2H_2 + O_2 \rightarrow HCO + HCO$

(45) $C_2H_2 + M \rightarrow C_2H + H$

These reactions were carried over from the kinetic mechanisms for acetylene and ethylene from reference 5.

CONCLUDING REMARKS

The stoichiometric combustion of propane behind incident shock waves was studied experimentally and analytically over a temperature range from 1700 K to 2600 K and a pressure range from 1.2 to 1.9 atm. Measurements of the concentrations of carbon monoxide [CO] and carbon dioxide [CO_2] and the product of the oxygen atom and carbon monoxide concentrations were made after passage of the incident shock wave. Analytical comparisons with the experimental data were made using a computer model of a flowing, reacting gas behind incident shock waves. In order to use the analytical model, a kinetic mechanism was assembled based on the assumption that propane decomposes rapidly to fragments with lower molecular weights followed by the oxidation of these fragments. A parametric study identifying and adjusting the rate coefficients of the reaction steps most sensitive in predicting the [O] [CO] concentration product, reaction times, and ignition delay times led to a kinetic mechanism which predicted well all present experimental results and experimental ignition delay times of a previous shock-tube study. The agreement between the computed and measured ignition delay times was also good. The kinetic mechanism, and associated rate coefficients, consists of 59 steps. Almost all the rate coefficients were taken from the literature.

The assumption that the parent hydrocarbon, propane in this case, decomposes rapidly to fragments with lower molecular weights followed by the oxidation of these fragments during later stages of the combustion process appears to be a valid approach. Since recent literature suggests that high-molecular-weight hydrocarbons such as iso-octane, toluene, and cyclohexane tend to follow this type of reaction sequence, there is a need to determine whether similar kinetic models can be assembled for these fuels.

Langley Research Center
National Aeronautics and Space Administration
Hampton, VA 23665
May 18, 1977

REFERENCES

1. Orr, C. R.: Combustion of Hydrocarbons Behind a Shock Wave. Ninth Symposium (International) on Combustion, Academic Press, Inc., 1963, pp. 1034-1045.

2. Cooke, D. F.; and Williams, Alan: Shock-Tube Studies of the Ignition and Combustion of Ethane and Slightly Rich Methane Mixtures With Oxygen. Thirteenth Symposium (International) on Combustion, Combustion Inst., 1971, pp. 757-766.

3. Cooke, D. F.; and Williams, Alan: Shock Tube Studies of Methane and Ethane Oxidation. Combust. & Flame, vol. 24, no. 2, Apr. 1975, pp. 245-256.

4. Jachimowski, Casimir J.: Kinetics of Oxygen Atom Formation During the Oxidation of Methane Behind Shock Waves. Combust. & Flame, vol. 23, no. 2, Oct. 1974, pp. 233-248.

5. Jachimowski, Casimir J.: An Experimental and Analytical Study of Acetylene and Ethylene Oxidation Behind Shock Waves. Combust. & Flame, vol. 29, no. 1, May 1977, pp. 55-66.

6. Burcat, Alexander; Lifshitz, Assa; Scheller, Karl; and Skinner, Gordon B.: Shock-Tube Investigation of Ignition in Propane-Oxygen-Argon Mixtures. Thirteenth Symposium (International) on Combustion, Combustion Inst., 1971, pp. 745-755.

7. Burcat, Alexander; Scheller, Karl; and Lifshitz, Assa: Shock-Tube Investigation of Comparative Ignition Delay Times for C_1-C_5 Alkanes. Combust. & Flame, vol. 16, no. 1, Feb. 1971, pp. 29-33.

8. Lifshitz, Assa; and Frenklach, Michael: Mechanism of the High Temperature Decomposition of Propane. J. Phys. Chem., vol. 79, no. 7, Mar. 27, 1975, pp. 686-692.

9. Leathard, D. A.; and Purnell, J. H.: The Self-Inhibited Pyrolysis of Propane at Small Extents of Reaction. Proc. R. Soc. (London), ser. A, vol. 305, no. 1483, July 23, 1968, pp. 517-540.

10. Myers, B. F.; and Bartle, E. R.: Reaction and Ignition Delay Times in the Oxidation of Propane. AIAA J., vol. 7, no. 10, Oct. 1969, pp. 1862-1869.

11. Chinitz, W.; and Baurer, T.: An Analysis of Nonequilibrium Hydrocarbon/Air Combustion. Pyrodynamics, vol. 4, no. 2, Apr. 1966, pp. 119-154.

12. Bittker, David A.; and Scullin, Vincent J.: General Chemical Kinetics Computer Program for Static and Flow Reactions, With Application to Combustion and Shock-Tube Kinetics. NASA TN D-6586, 1972.

13. Baulch, D. L.; Drysdale, D. D.; Horne, D. G.; and Lloyd, A. C.: Evaluated Kinetic Data for High Temperature Reactions. Volume I - Homogeneous Gas Phase Reactions of the H_2-O_2 System. CRC Press, c.1972.

14. Benson, Sidney W.; and O'Neal, H. Edward: Kinetic Data on Gas Phase Unimolecular Reactions. NSRDS-NBS 21, U.S. Dep. Commer., Feb. 1970.

15. Drysdale, D. D.; and Lloyd, A. C.: Gas Phase Reactions of the Hydroxyl Radical. Oxid. & Combust. Rev., vol. 4, 1969, pp. 157-250.

16. Semenov, N. N. (Michel Boudart, transl.): Some Problems in Chemical Kinetics and Reactivity. Volume 1. Princeton Univ. Press, 1959.

17. McLain, Allen G.; and Rao, C. S. R.: A Hybrid Computer Program for Rapidly Solving Flowing or Static Chemical Kinetic Problems Involving Many Chemical Species. NASA TM X-3403, 1976.

18. JANAF Thermochemical Tables. Second Ed. NSRDS-NBS 37, U.S. Dep. Commer., June 1971.

19. Bahn, Gilbert S.: Approximate Thermochemical Tables for Some C-H and C-H-O Species. NASA CR-2178, 1973.

20. Hartig, R.; Troe, J.; and Wagner, H. Gg.: Thermal Decomposition of Methane Behind Reflected Shock Waves. Thirteenth Symposium (International) on Combustion, Combustion Inst., 1971, pp. 147-154.

21. Bowman, Craig T.: A Shock-Tube Investigation of the High-Temperature Oxidation of Methanol. Combust. & Flame, vol. 25, no. 3, Dec. 1975, pp. 343-354.

22. Vandooren, J.; Peeters, J.; and Van Tiggelen, P. J.: Rate Constant of the Elementary Reaction of Carbon Monoxide With Hydroxyl Radical. Fifteenth Symposium (International) on Combustion, Combustion Inst., c.1975, pp. 745-753.

TABLE I.- EXPERIMENTAL RESULTS

(a) At observation station ①

T, K	p, atm	[O][CO], $(mol/cm^3)^2$	t_m, μsec	$[CO_2]$, mol/cm^3	[CO], mol/cm^3	T_m, K
2525	1.81	9.70×10^{-15}	4.0	----	1.69×10^{-7}	2710
2522	1.81	9.70	4.0	----	1.70	2709
2510	1.80	10.2	4.0	----	1.71	2697
2510	1.80	11.2	4.0	4.40×10^{-8}	----	2697
2505	1.80	96.7	4.0	4.59	----	2692
2470	1.77	10.4	4.0	4.30	----	2660
2422	1.74	11.2	4.0	4.62	----	2616
2296	1.62	----	---	4.58	----	2503
2277	1.60	----	---	----	1.79	2486
2247	1.59	8.65	5.0	4.89	----	2459
2247	1.59	8.59	5.0	4.46	----	2459
2235	1.56	8.76	6.0	----	1.76	2448
2073	1.44	6.82	9.0	----	1.67	2309
1987	1.37	7.44	9.5	----	1.83	2237
1887	1.28	5.64	10.0	----	1.34	2157
1887	1.28	5.60	12.5	3.76	----	2157
1880	1.28	6.53	12.0	----	1.52	2152
1874	1.27	5.92	11.0	3.85	----	2146
1870	1.27	5.57	11.0	3.83	----	2143
1862	1.26	6.38	10.0	----	1.55	2137

TABLE I.- Concluded

(b) At observation station ②

T, K	p, atm	$[O][CO]$, $(mol/cm^3)^2$	t_m, μsec	$[CO_2]$, mol/cm^3	$[CO]$, mol/cm^3	T_m, K
2615	1.90	10.5×10^{-15}	3.50	4.45×10^{-8}	1.48×10^{-7}	2793
2570	1.86	9.18	2.80	4.20	1.49	2751
2480	1.77	10.1	4.00	4.76	1.74	2670
2415	1.71	8.99	3.50	4.24	1.55	2611
2300	1.61	8.72	5.50	4.15	1.72	2507
2300	1.61	8.21	-----	3.78	1.61	2507
2255	1.57	8.31	5.50	4.26	1.72	2467
2170	1.50	8.50	7.50	4.07	1.77	2392
2180	1.51	7.95	7.00	3.68	1.72	2401
2005	1.37	8.38	10.0	4.07	1.48	2254
1190	1.36	7.86	9.00	4.12	1.65	2240
1895	1.28	6.82	12.0	3.65	1.63	2165
1805	1.21	6.31	-----	3.88	1.74	2095

TABLE II.- PRELIMINARY KINETIC MECHANISM FOR PROPANE COMBUSTION

	Reaction	Rate coefficient, k (a)	Ref.
(1)	$C_3H_8 \rightarrow CH_3 + C_2H_5$	$5.00 \times 10^{15} \exp(-43\ 785/T)$	Estimated
(2)	$CH_3 + C_3H_8 \rightarrow CH_4 + n\text{-}C_3H_7$	$3.55 \times 10^{12} \exp(-5184/T)$	8
(3)	$CH_3 + C_3H_8 \rightarrow CH_4 + i\text{-}C_3H_7$	$3.55 \times 10^{12} \exp(-5184/T)$	8
(4)	$H + C_3H_8 \rightarrow H_2 + n\text{-}C_3H_7$	$6.30 \times 10^{13} \exp(-4026/T)$	8
(5)	$H + C_3H_8 \rightarrow H_2 + i\text{-}C_3H_7$	$6.30 \times 10^{13} \exp(-4026/T)$	8
(6)	$O + C_3H_8 \rightarrow OH + n\text{-}C_3H_7$	$5.00 \times 10^{13} \exp(-5033/T)$	Estimated
(7)	$O + C_3H_8 \rightarrow OH + i\text{-}C_3H_7$	$5.00 \times 10^{13} \exp(-5033/T)$	Estimated
(8)	$OH + C_3H_8 \rightarrow H_2O + n\text{-}C_3H_7$	$1.60 \times 10^{14} \exp(-1580/T)$	15
(9)	$OH + C_3H_8 \rightarrow H_2O + i\text{-}C_3H_7$	$1.60 \times 10^{14} \exp(-1580/T)$	15
(10)	$n\text{-}C_3H_7 \rightarrow C_2H_4 + CH_3$	$4.00 \times 10^{13} \exp(-16\ 658/T)$	14
(11)	$i\text{-}C_3H_7 \rightarrow C_2H_4 + CH_3$	$1.00 \times 10^{12} \exp(-17\ 363/T)$	8
(12)	$n\text{-}C_3H_7 \rightarrow C_3H_6 + H$	$6.30 \times 10^{13} \exp(-19\ 124/T)$	14
(13)	$i\text{-}C_3H_7 \rightarrow C_3H_6 + H$	$2.00 \times 10^{14} \exp(-20\ 785/T)$	14
(14)	$O + C_3H_6 \rightarrow CH_2O + C_2H_4$	1.00×10^{13}	Estimated
(15)	$M + H + O_2 \rightarrow HO_2 + M$	$1.50 \times 10^{15} \exp(500/T)$	13
(16)	$M + CH_4 \rightarrow CH_3 + H + M$	$4.00 \times 10^{17} \exp(-44\ 500/T)$	4
(17)	$CH_4 + H \rightarrow CH_3 + H_2$	$1.26 \times 10^{14} \exp(-5989/T)$	4
(18)	$CH_4 + OH \rightarrow CH_3 + H_2O$	$3.00 \times 10^{13} \exp(-3020/T)$	4
(19)	$CH_4 + O \rightarrow CH_3 + OH$	$2.00 \times 10^{13} \exp(-4640/T)$	4

[a]The units for k are sec^{-1} for unimolecular reactions, $cm^3/mol\text{-}sec$ for bimolecular reactions, and $cm^6/mol^2\text{-}sec$ for termolecular reactions.

TABLE II.- Continued

Reaction	Rate coefficient, k (a)	Ref.
(20) $CH_3 + O_2 \rightarrow CH_2O + OH$	$1.70 \times 10^{12} \exp(-7045/T)$	4
(21) $CH_3 + O \rightarrow CH_2O + H$	$1.30 \times 10^{14} \exp(-1006/T)$	4
(22) $CH_2O + OH \rightarrow HCO + H_2O$	2.30×10^{13}	4, 5
(23) $HCO + OH \rightarrow CO + H_2O$	1.00×10^{14}	5
(24) $M + HCO \rightarrow H + CO + M$	$5.00 \times 10^{14} \exp(-9562/T)$	5
(25) $CO + OH \rightarrow CO_2 + H$	$4.00 \times 10^{12} \exp(-4026/T)$	4, 5
(26) $CO + O + M \rightarrow CO_2 + M$	6.00×10^{13}	5
(27) $O + H_2 \rightarrow OH + H$	$2.07 \times 10^{14} \exp(-6920/T)$	4, 5
(28) $H + O_2 \rightarrow OH + O$	$1.22 \times 10^{17} T^{-0.91} \exp(-8369/T)$	4, 5
(29) $H_2 + OH \rightarrow H_2O + H$	$5.20 \times 10^{13} \exp(-3271/T)$	4, 5
(30) $OH + OH \rightarrow H_2O + O$	$5.50 \times 10^{13} \exp(-3523/T)$	4, 5
(31) $H + H + M \rightarrow H_2 + M$	1.00×10^{15}	5
(32) $H + OH + M \rightarrow H_2O + M$	$8.40 \times 10^{21} T^{-2.0}$	4, 5
(33) $O_2 + H_2 \rightarrow OH + OH$	$1.70 \times 10^{13} \exp(-24\ 230/T)$	4
(34) $M + O_2 \rightarrow O + O + M$	$2.55 \times 10^{18} T^{-1.0} \exp(-59\ 386/T)$	4, 5
(35) $M + C_2H_4 \rightarrow C_2H_3 + H + M$	$1.00 \times 10^{14} \exp(-54\ 857/T)$	5
(36) $C_2H_4 + C_2H_4 \rightarrow C_2H_5 + C_2H_3$	$5.00 \times 10^{14} \exp(-32\ 562/T)$	5
(37) $C_2H_5 \rightarrow C_2H_4 + H$	$3.16 \times 10^{13} \exp(-20\ 483/T)$	5
(38) $M + C_2H_3 \rightarrow C_2H_2 + H + M$	$3.00 \times 10^{16} \exp(-20\ 382/T)$	5

[a]The units for k are sec^{-1} for unimolecular reactions, $cm^3/mol\text{-}sec$ for bimolecular reactions, and $cm^6/mol^2\text{-}sec$ for termolecular reactions.

TABLE II.- Concluded

	Reaction	Rate coefficient, k (a)	Ref.
(39)	$H + C_2H_4 \rightarrow C_2H_3 + H_2$	$1.10 \times 10^{14} \exp(-4278/T)$	5
(40)	$OH + C_2H_4 \rightarrow C_2H_3 + H_2O$	$1.00 \times 10^{14} \exp(-1761/T)$	5
(41)	$O + C_2H_4 \rightarrow CH_2O + CH_2$	$2.50 \times 10^{13} \exp(-2516/T)$	5
(42)	$O + C_2H_4 \rightarrow CH_3 + HCO$	$2.26 \times 10^{13} \exp(-1359/T)$	5
(43)	$CH_2O + H \rightarrow HCO + H_2$	2.00×10^{13}	5
(44)	$CH_2O + O \rightarrow HCO + OH$	2.00×10^{13}	5
(45)	$M + C_2H_2 \rightarrow C_2H + H + M$	$1.00 \times 10^{14} \exp(-57\ 373/T)$	5
(46)	$C_2H_2 + O_2 \rightarrow HCO + HCO$	$4.00 \times 10^{12} \exp(-14\ 092/T)$	5
(47)	$H + C_2H_2 \rightarrow C_2H + H_2$	$2.00 \times 10^{14} \exp(-9562/T)$	5
(48)	$OH + C_2H_2 \rightarrow C_2H + H_2O$	$6.00 \times 10^{12} \exp(-3523/T)$	5
(49)	$O + C_2H_2 \rightarrow C_2H + OH$	$3.20 \times 10^{15} T^{-0.6} \exp(-8556/T)$	5
(50)	$O + C_2H_2 \rightarrow CH_2 + CO$	$5.20 \times 10^{13} \exp(-1862/T)$	5
(51)	$C_2H + O_2 \rightarrow HCO + CO$	$1.00 \times 10^{13} \exp(-3523/T)$	5
(52)	$C_2H + O \rightarrow CO + CH$	5.00×10^{13}	5
(53)	$CH_2 + O_2 \rightarrow HCO + OH$	$1.00 \times 10^{14} \exp(-1862/T)$	5
(54)	$CH + O_2 \rightarrow CO + OH$	$1.35 \times 10^{11} T^{0.67} \exp(-12\ 934/T)$	5
(55)	$CH + O_2 \rightarrow HCO + O$	1.00×10^{13}	5
(56)	$HCO + H \rightarrow CO + H_2$	1.00×10^{14}	5
(57)	$HCO + O \rightarrow CO + OH$	1.26×10^{14}	5

[a]The units for k are sec^{-1} for unimolecular reactions, $cm^3/mol\text{-}sec$ for bimolecular reactions, and $cm^6/mol^2\text{-}sec$ for termolecular reactions.

TABLE III.- FINAL KINETIC MECHANISM FOR PROPANE COMBUSTION

	Reaction	Rate coefficient, k (a)	Ref.
(1)	$M + C_3H_8 \rightarrow C_2H_5 + CH_3 + M$	$5.00 \times 10^{15} \exp(-32\ 713/T)$	Present study
(2)	$CH_3 + C_3H_8 \rightarrow CH_4 + n\text{-}C_3H_7$	$2.00 \times 10^{13} \exp(-5184)/T)$	Present study
(3)	$CH_3 + C_3H_8 \rightarrow CH_4 + i\text{-}C_3H_7$	$2.00 \times 10^{13} \exp(-5184)/T)$	Present study
(4)	$H + C_3H_8 \rightarrow H_2 + n\text{-}C_3H_7$	$6.30 \times 10^{13} \exp(-4026/T)$	8
(5)	$H + C_3H_8 \rightarrow H_2 + i\text{-}C_3H_7$	$6.30 \times 10^{13} \exp(-4026/T)$	8
(6)	$O + C_3H_8 \rightarrow OH + n\text{-}C_8H_7$	$5.00 \times 10^{13} \exp(-5033/T)$	Estimated
(7)	$O + C_3H_8 \rightarrow OH + i\text{-}C_3H_7$	$5.00 \times 10^{13} \exp(-5033/T)$	Estimated
(8)	$OH + C_3H_8 \rightarrow H_2O + n\text{-}C_3H_7$	$1.60 \times 10^{14} \exp(-1580/T)$	15
(9)	$OH + C_3H_8 \rightarrow H_2O + i\text{-}C_3H_7$	$1.60 \times 10^{14} \exp(-1580/T)$	15
(10)	$n\text{-}C_3H_7 \rightarrow C_2H_4 + CH_3$	$4.00 \times 10^{13} \exp(-16\ 658/T)$	14
(11)	$i\text{-}C_3H_7 \rightarrow C_2H_4 + CH_3$	$1.00 \times 10^{12} \exp(-17\ 363/T)$	8
(12)	$n\text{-}C_3H_7 \rightarrow C_3H_6 + H$	$6.30 \times 10^{13} \exp(-19\ 124/T)$	14
(13)	$i\text{-}C_3H_7 \rightarrow C_3H_6 + H$	$2.00 \times 10^{14} \exp(-20\ 785/T)$	14
(14)	$O + C_3H_6 \rightarrow CH_2O + C_2H_4$	1.00×10^{13}	Estimated
(15)	$M + H + O_2 \rightarrow HO_2 + M$	$1.50 \times 10^{15} \exp(500/T)$	13
(16)	$M + CH_4 \rightarrow CH_3 + H + M$	$4.00 \times 10^{17} \exp(-44\ 500/T)$	4
(17)	$CH_4 + H \rightarrow CH_3 + H_2$	$1.26 \times 10^{14} \exp(-5989/T)$	4
(18)	$CH_4 + OH \rightarrow CH_3 + H_2O$	$3.00 \times 10^{13} \exp(-3020/T)$	4
(19)	$CH_4 + O \rightarrow CH_3 + OH$	$2.00 \times 10^{13} \exp(-4640/T)$	4

[a]The units for k are sec^{-1} for unimolecular reactions, $cm^3/mol\text{-}sec$ for bimolecular reactions, and $cm^6/mol^2\text{-}sec$ for termolecular reactions.

TABLE III.- Continued

	Reaction	Rate coefficient, k (a)	Ref.
(20)	$CH_3 + O_2 \rightarrow CH_2O + OH$	$1.70 \times 10^{12} \exp(-7045/T)$	4
(21)	$CH_3 + O \rightarrow CH_2O + H$	$1.30 \times 10^{14} \exp(-1006/T)$	4
(22)	$CH_2O + OH \rightarrow HCO + H_2O$	2.30×10^{13}	4, 5
(23)	$HCO + OH \rightarrow CO + H_2O$	1.00×10^{14}	5
(24)	$M + HCO \rightarrow H + CO + M$	$5.00 \times 10^{14} \exp(-9562/T)$	5
(25)	$CO + OH \rightarrow CO_2 + H$	$4.00 \times 10^{12} \exp(-4026/T)$	4, 5
(26)	$CO + O + M \rightarrow CO_2 + M$	6.00×10^{13}	5
(27)	$O + H_2 \rightarrow OH + H$	$2.07 \times 10^{14} \exp(-6920/T)$	4, 5
(28)	$H + O_2 \rightarrow OH + O$	$1.22 \times 10^{17}T^{-0.91} \exp(-8369/T)$	4, 5
(29)	$H_2 + OH \rightarrow H_2O + H$	$5.20 \times 10^{13} \exp(-3271/T)$	4, 5
(30)	$OH + OH \rightarrow H_2O + O$	$5.50 \times 10^{13} \exp(-3523/T)$	4, 5
(31)	$H + H + M \rightarrow H_2 + M$	1.00×10^{15}	5
(32)	$H + OH + M \rightarrow H_2O + M$	$8.40 \times 10^{21}T^{-2.0}$	4, 5
(33)	$O_2 + H_2 \rightarrow OH + OH$	$1.70 \times 10^{13} \exp(-24\ 230/T)$	4
(34)	$M + O_2 \rightarrow O + O + M$	$2.55 \times 10^{18}T^{-1.0} \exp(-59\ 386/T)$	4, 5
(35)	$M + C_2H_4 \rightarrow C_2H_3 + H + M$	$1.00 \times 10^{14} \exp(-54\ 857/T)$	5
(36)	$C_2H_4 + C_2H_4 \rightarrow C_2H_5 + C_2H_3$	$5.00 \times 10^{14} \exp(-32\ 562/T)$	5
(37)	$C_2H_5 \rightarrow C_2H_4 + H$	$3.16 \times 10^{13} \exp(-20\ 483/T)$	5
(38)	$M + C_2H_3 \rightarrow C_2H_2 + H + M$	$3.00 \times 10^{16} \exp(-20\ 382/T)$	5

[a]The units for k are sec^{-1} for unimolecular reactions, $cm^3/mol\text{-}sec$ for bimolecular reactions, and $cm^6/mol^2\text{-}sec$ for termolecular reactions.

TABLE III.- Concluded

	Reaction	Rate coefficient, k (a)	Ref.
(39)	$H + C_2H_4 \rightarrow C_2H_3 + H_2$	$1.10 \times 10^{14} \exp(-4278/T)$	5
(40)	$OH + C_2H_4 \rightarrow C_2H_3 + H_2O$	$1.00 \times 10^{14} \exp(-1761/T)$	5
(41)	$O + C_2H_4 \rightarrow CH_2O + CH_2$	$2.50 \times 10^{13} \exp(-2516/T)$	5
(42)	$O + C_2H_4 \rightarrow CH_3 + HCO$	$2.26 \times 10^{13} \exp(-1359/T)$	5
(43)	$CH_2O + H \rightarrow HCO + H_2$	2.00×10^{13}	5
(44)	$CH_2O + O \rightarrow HCO + OH$	2.00×10^{13}	5
(45)	$M + C_2H_2 \rightarrow C_2H + H + M$	$1.00 \times 10^{14} \exp(-57\ 373/T)$	5
(46)	$C_2H_2 + O_2 \rightarrow HCO + HCO$	$4.00 \times 10^{12} \exp(-14\ 092/T)$	5
(47)	$H + C_2H_2 \rightarrow C_2H + H_2$	$2.00 \times 10^{14} \exp(-9562/T)$	5
(48)	$OH + C_2H_2 \rightarrow C_2H + H_2O$	$6.00 \times 10^{12} \exp(-3523/T)$	5
(49)	$O + C_2H_2 \rightarrow C_2H + OH$	$3.20 \times 10^{15} T^{-0.6} \exp(-8556/T)$	5
(50)	$O + C_2H_2 \rightarrow CH_2 + CO$	$5.20 \times 10^{13} \exp(-1862/T)$	5
(51)	$C_2H + O_2 \rightarrow HCO + CO$	$1.00 \times 10^{13} \exp(-3523/T)$	5
(52)	$C_2H + O \rightarrow CO + CH$	5.00×10^{13}	5
(53)	$CH_2 + O_2 \rightarrow HCO + OH$	$1.00 \times 10^{14} \exp(-1862/T)$	5
(54)	$CH + O_2 \rightarrow CO + OH$	$1.35 \times 10^{11} T^{0.67} \exp(-12\ 934/T)$	5
(55)	$CH + O_2 \rightarrow HCO + O$	1.00×10^{13}	5
(56)	$HCO + H \rightarrow CO + H_2$	1.00×10^{14}	5
(57)	$HCO + O \rightarrow CO + OH$	1.26×10^{14}	5
(58)	$H + HO_2 \rightarrow OH + OH$	$2.50 \times 10^{14} \exp(-950/T)$	19
(59)	$CO + HO_2 \rightarrow OH + CO_2$	1.00×10^{10}	Estimated

[a]The units for k are sec^{-1} for unimolecular reactions, $cm^3/mol\text{-}sec$ for bimolecular reactions, and $cm^6/mol^2\text{-}sec$ for termolecular reactions.

TABLE IV.- COMPARISON BETWEEN MEASURED AND CALCULATED IGNITION TIMES

Gas composition, percent mole			T, K	p, atm	t_i, μsec	
C_3H_8	O_2	Ar			Measured (a)	Calculated
1.60	8.00	90.40	1327	8.59	282	320
1.60	8.00	90.40	1352	8.45	185	220
.80	8.00	91.20	1423	7.66	70	65
1.60	4.00	94.40	1447	8.10	225	300
.41	4.10	95.49	1492	7.67	77	60
1.60	8.00	90.40	1495	2.62	68	75
.84	2.10	97.06	1539	8.32	230	230
3.85	19.23	76.92	1587	14.07	12	10

[a]From reference 6.

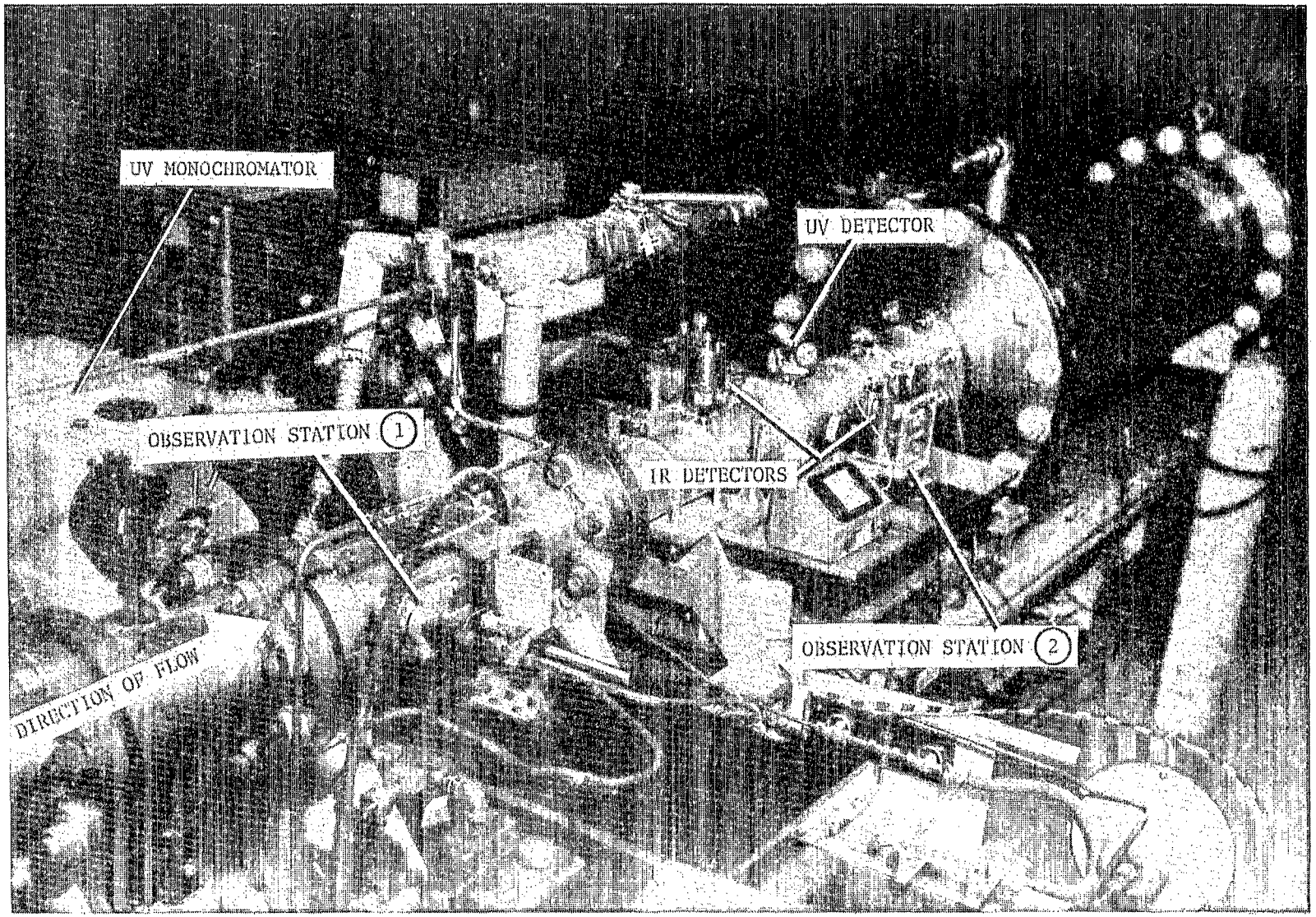

L-77-2279.1

Figure 1.- Photograph of shock tube indicating location of test observation stations.

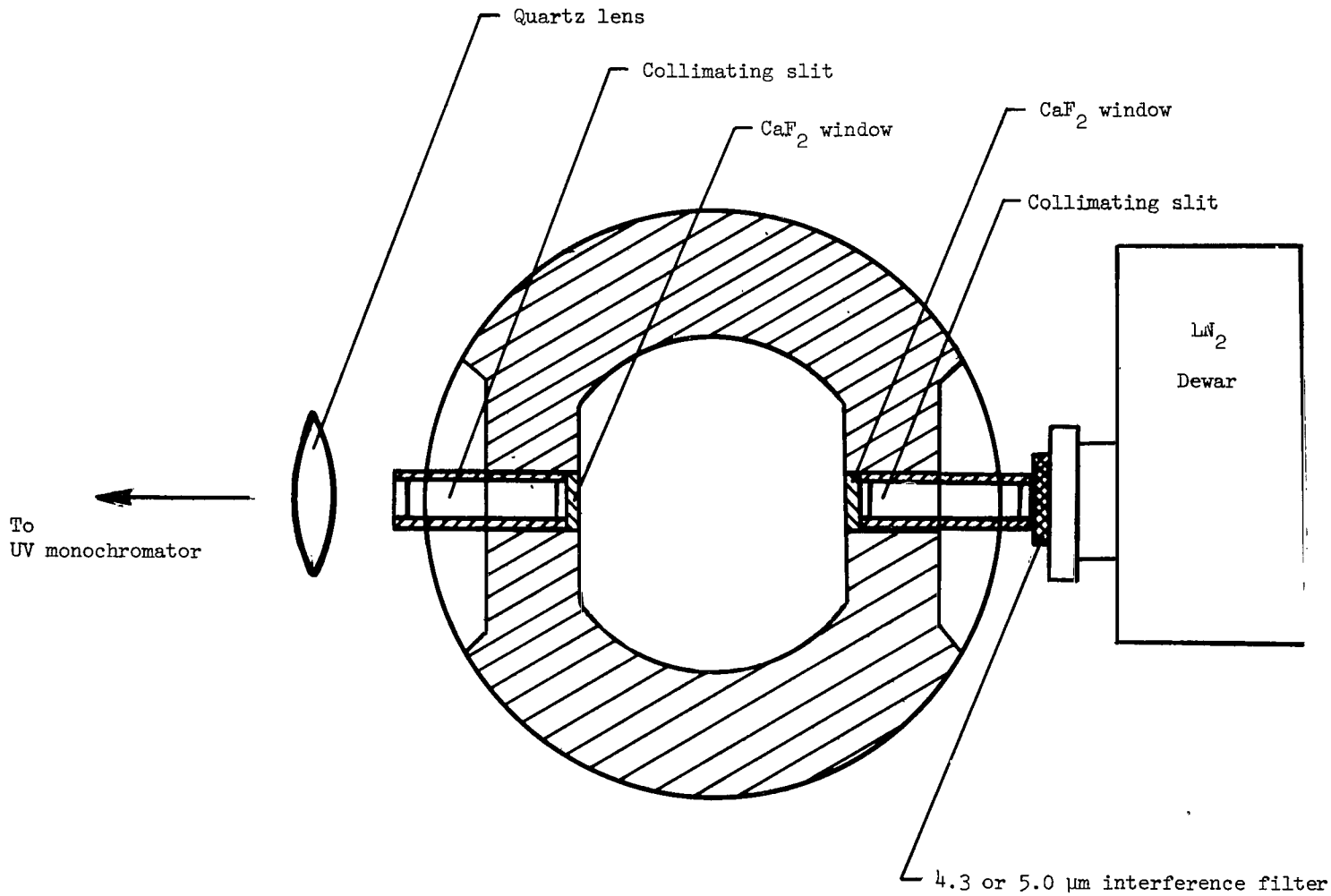

(a) Observation station ①.

Figure 2.- Schematic representation of instrumentation arrangement at observation stations.

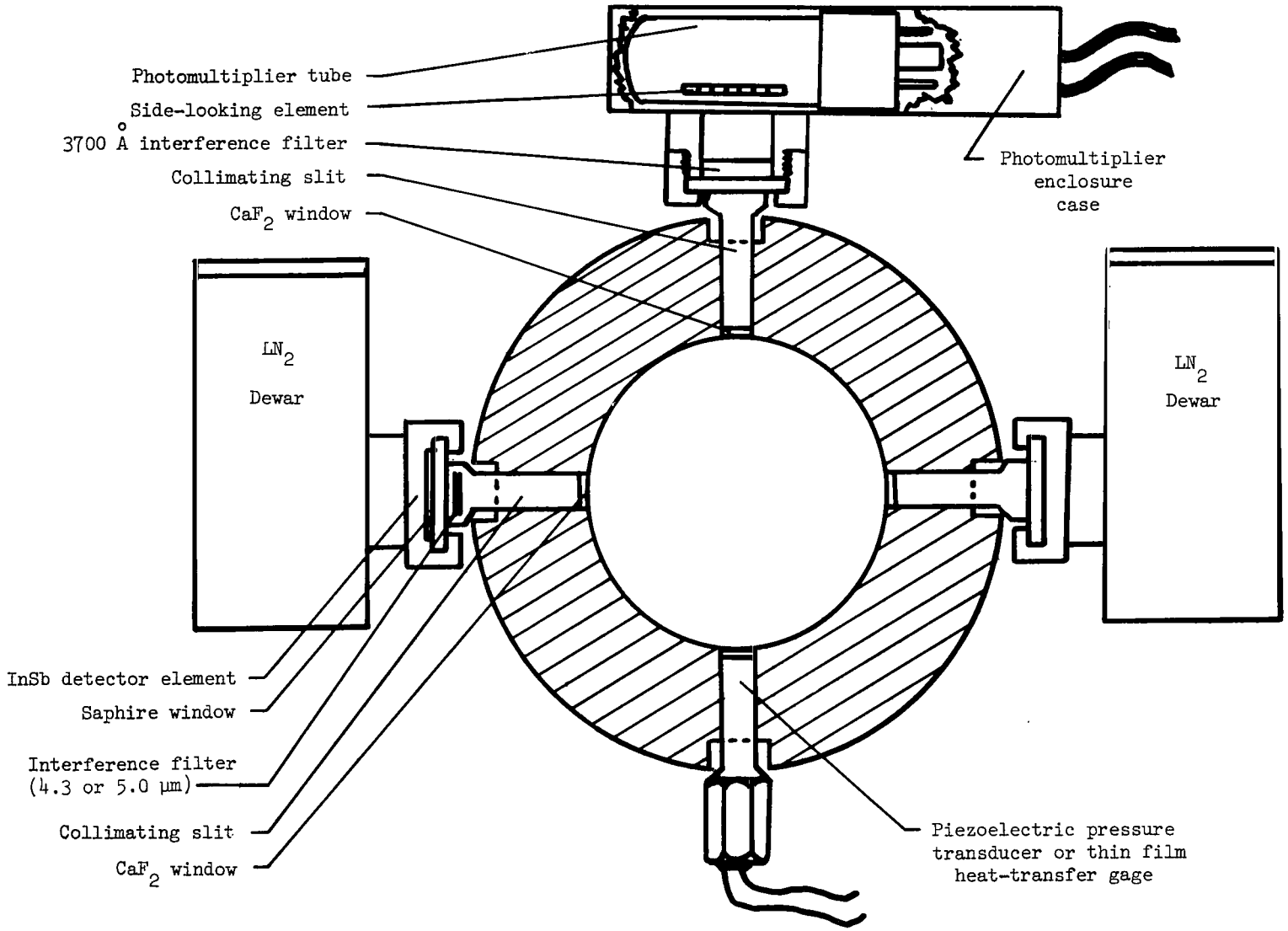

(b) Observation station ②.

Figure 2.- Concluded.

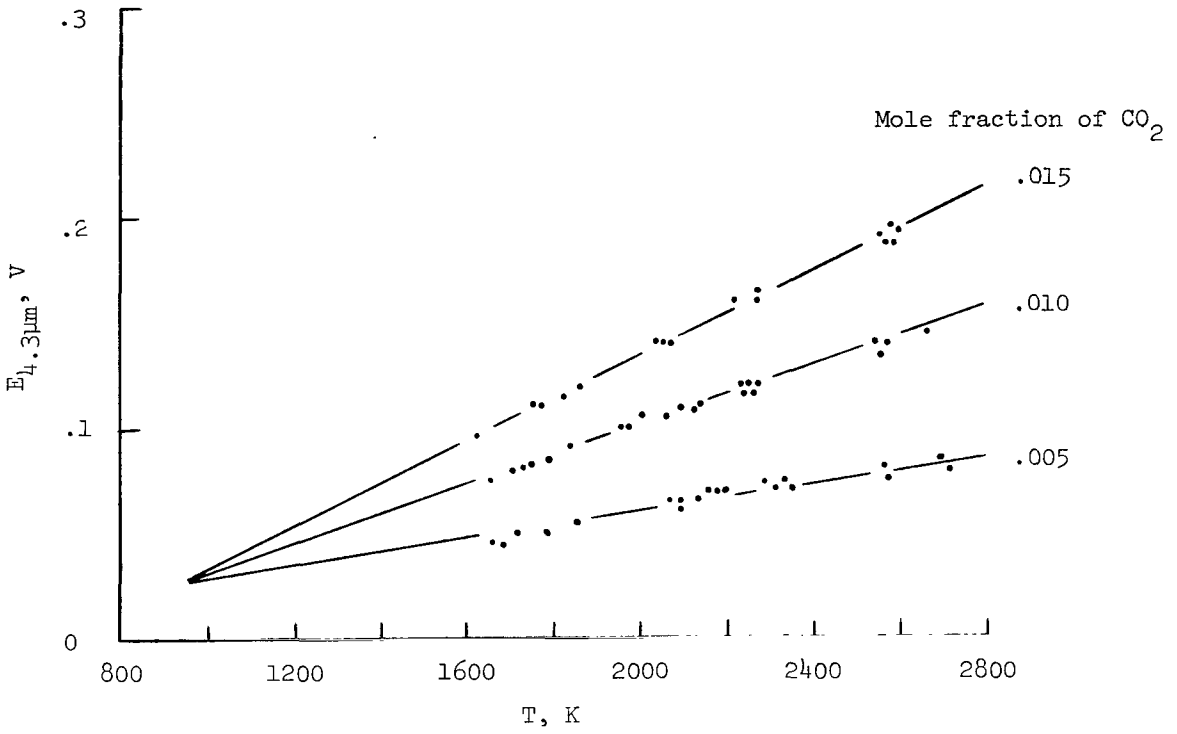

(a) Variation of CO_2 emission voltage at 4.3 μm with temperature.

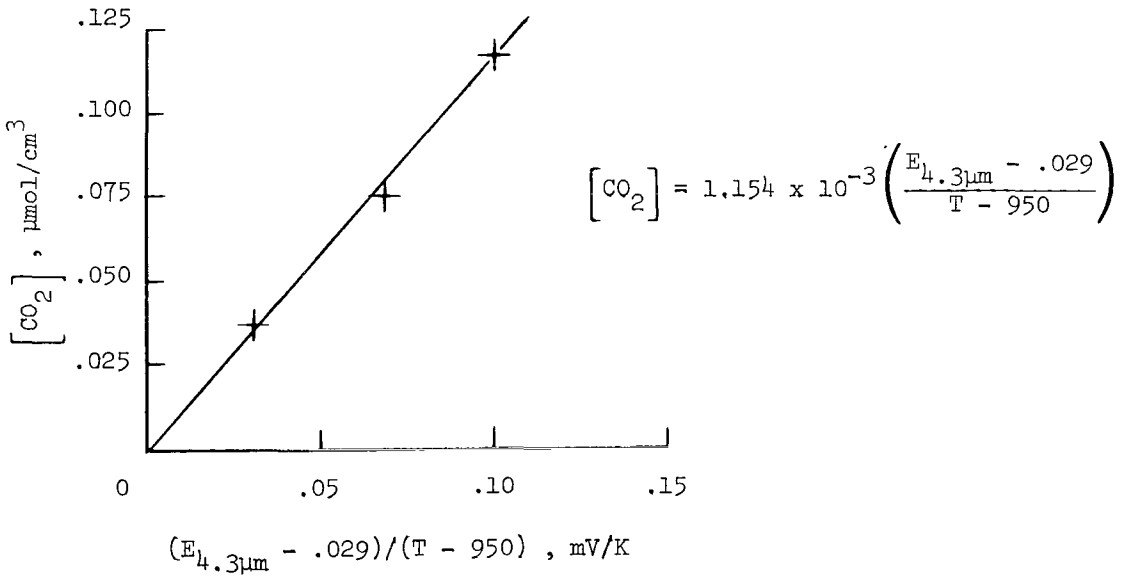

(b) Correlation of molar concentration with temperature and emission voltage.

Figure 3.- Calibration of detection system for obtaining CO_2 molar concentration, $[CO_2]$.

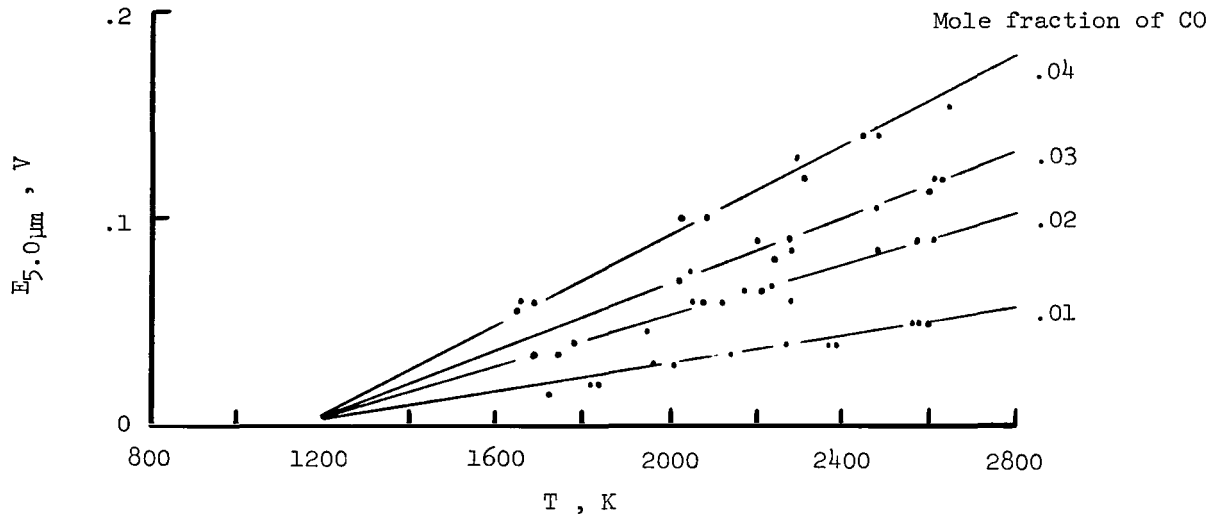

(a) Variation of CO emission voltage at 5.0 μm with temperature.

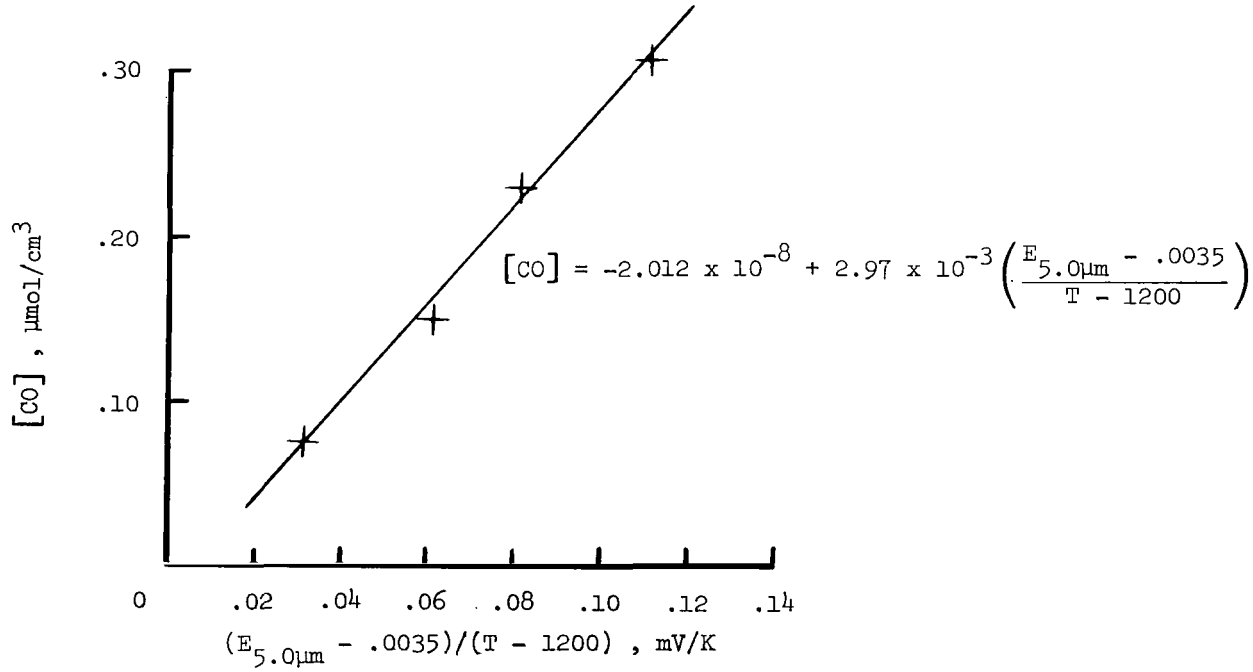

(b) Correlation of molar concentration with temperature and emission voltage.

Figure 4.- Calibration of detection system for obtaining CO molar concentration, [CO].

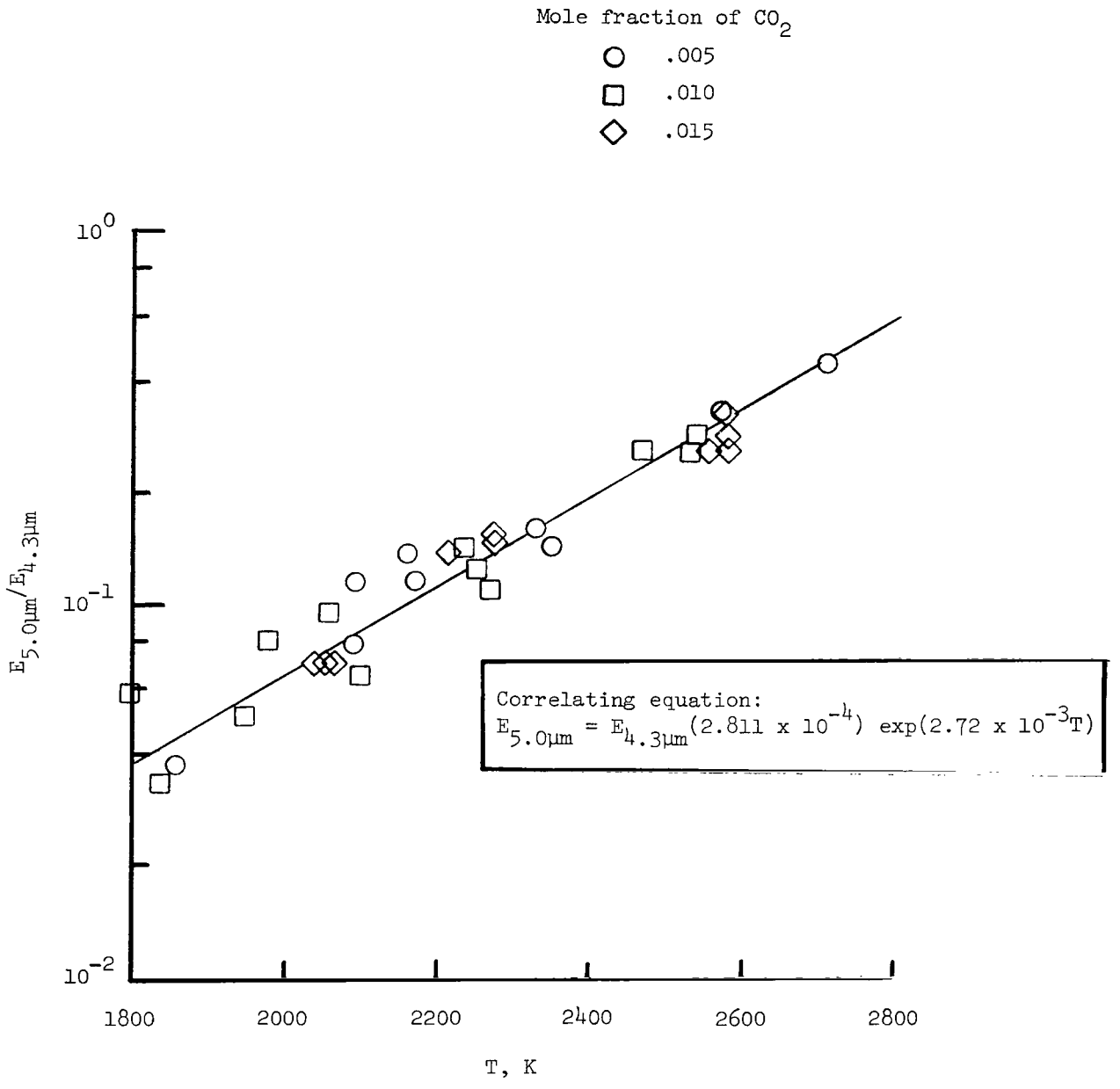

Figure 5.- Correction of CO emission voltage for CO_2 emission interference at 5.0 μm.

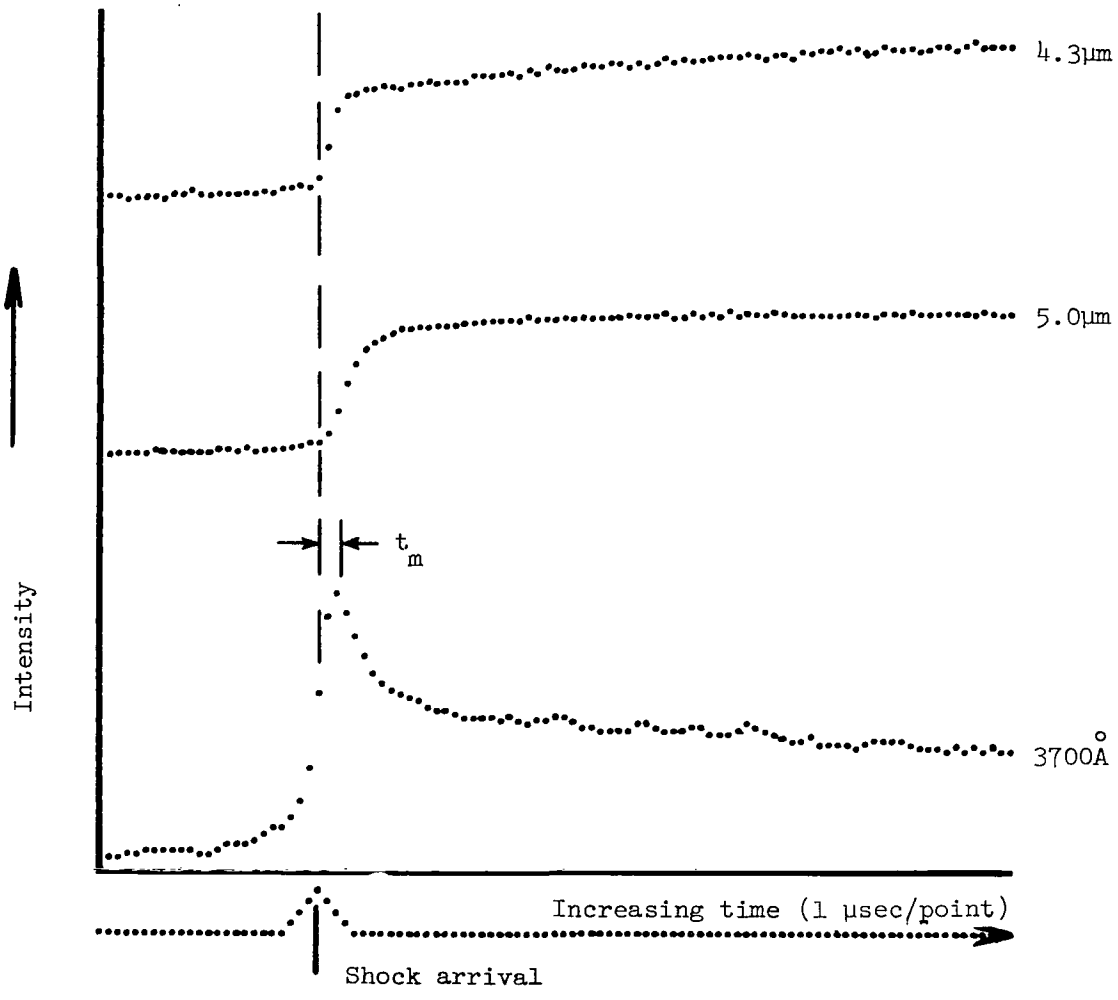

Figure 6.- Typical emission profiles at 4.3 μm, 5.0 μm, and 3700 Å.

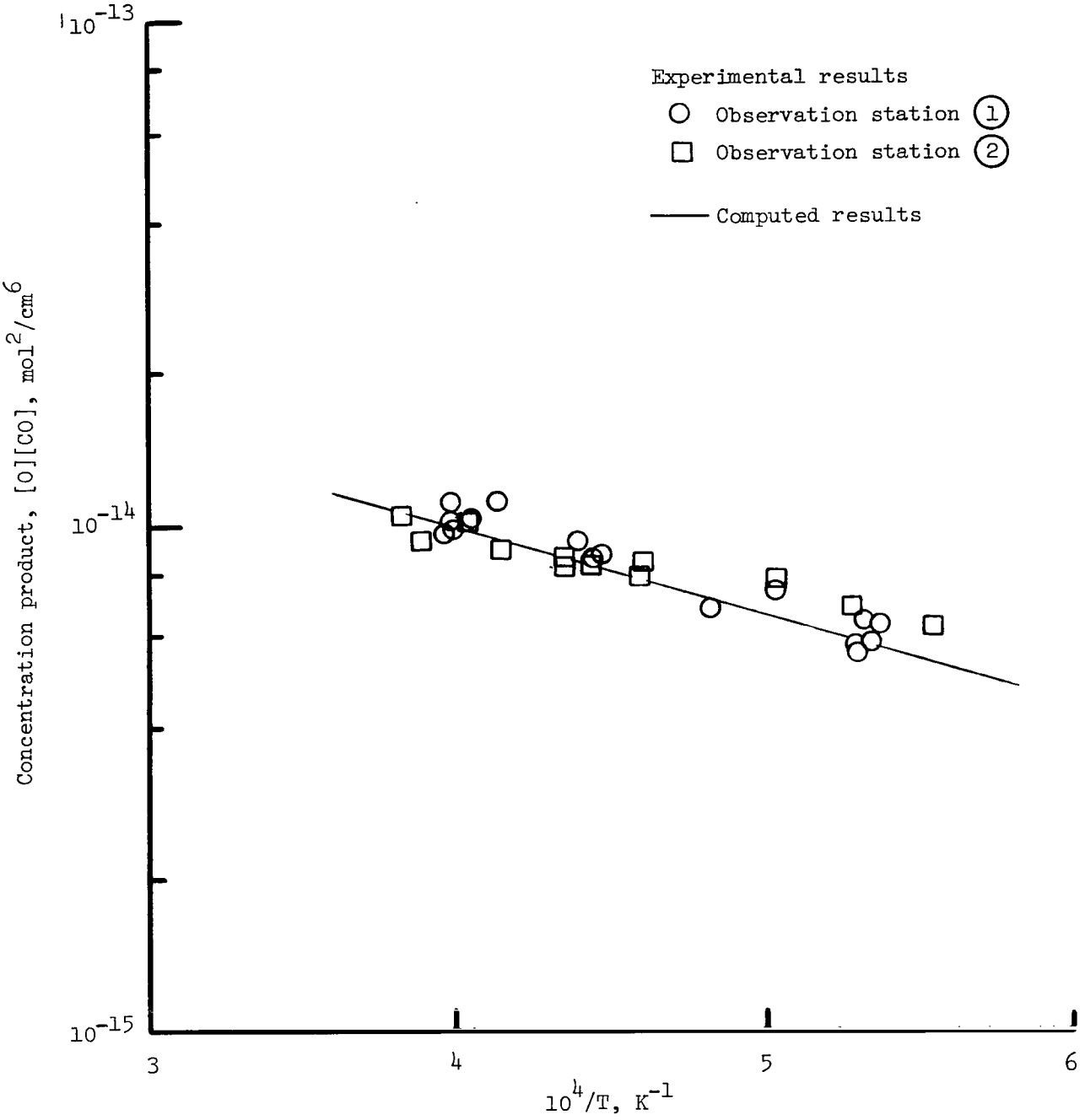

Figure 7.- Comparison of predicted and measured [O][CO] values from stoichiometric propane combustion.

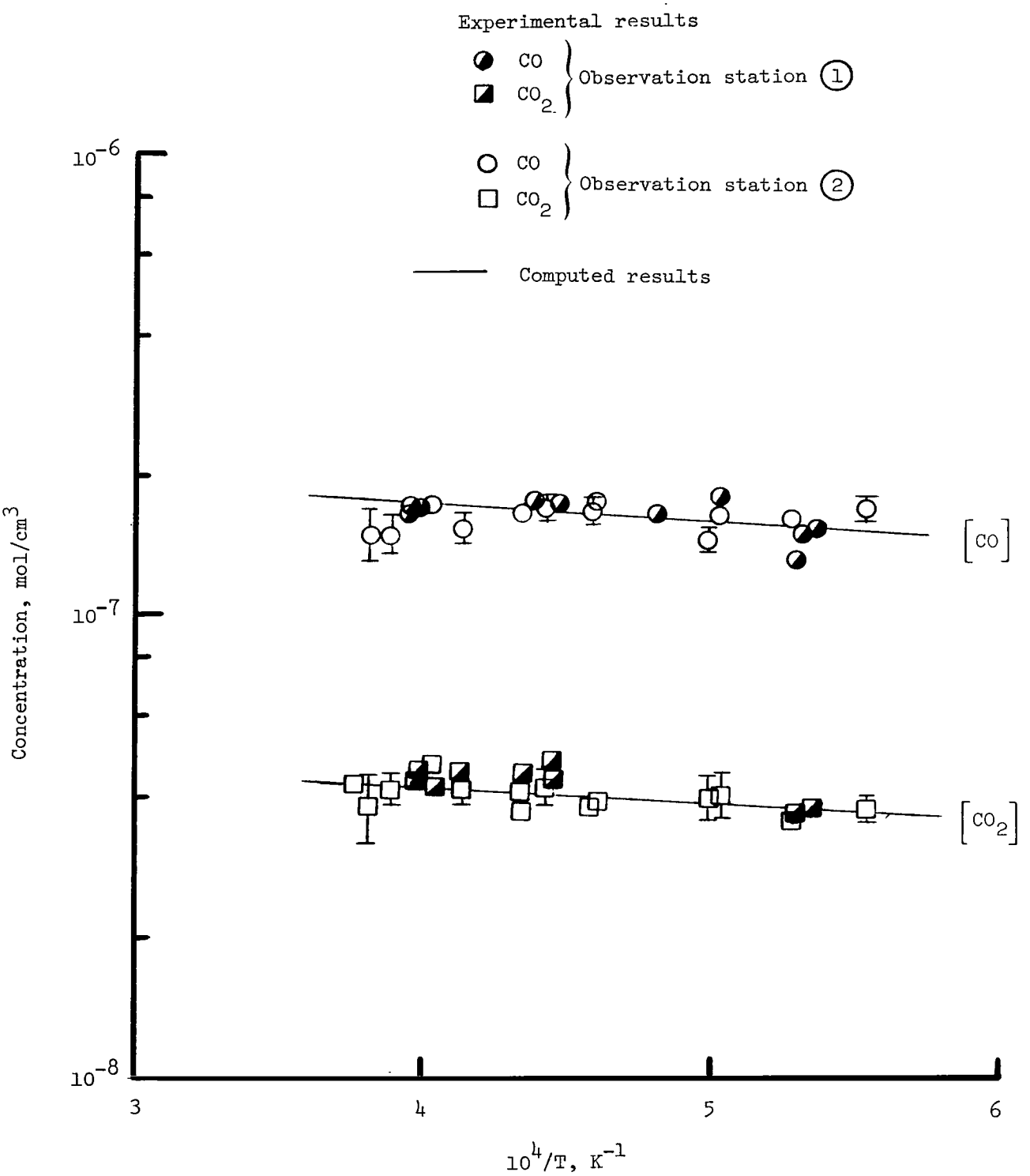

Figure 8.- Comparison of predicted and measured molar concentrations of CO and CO_2 during stoichiometric combustion of propane.

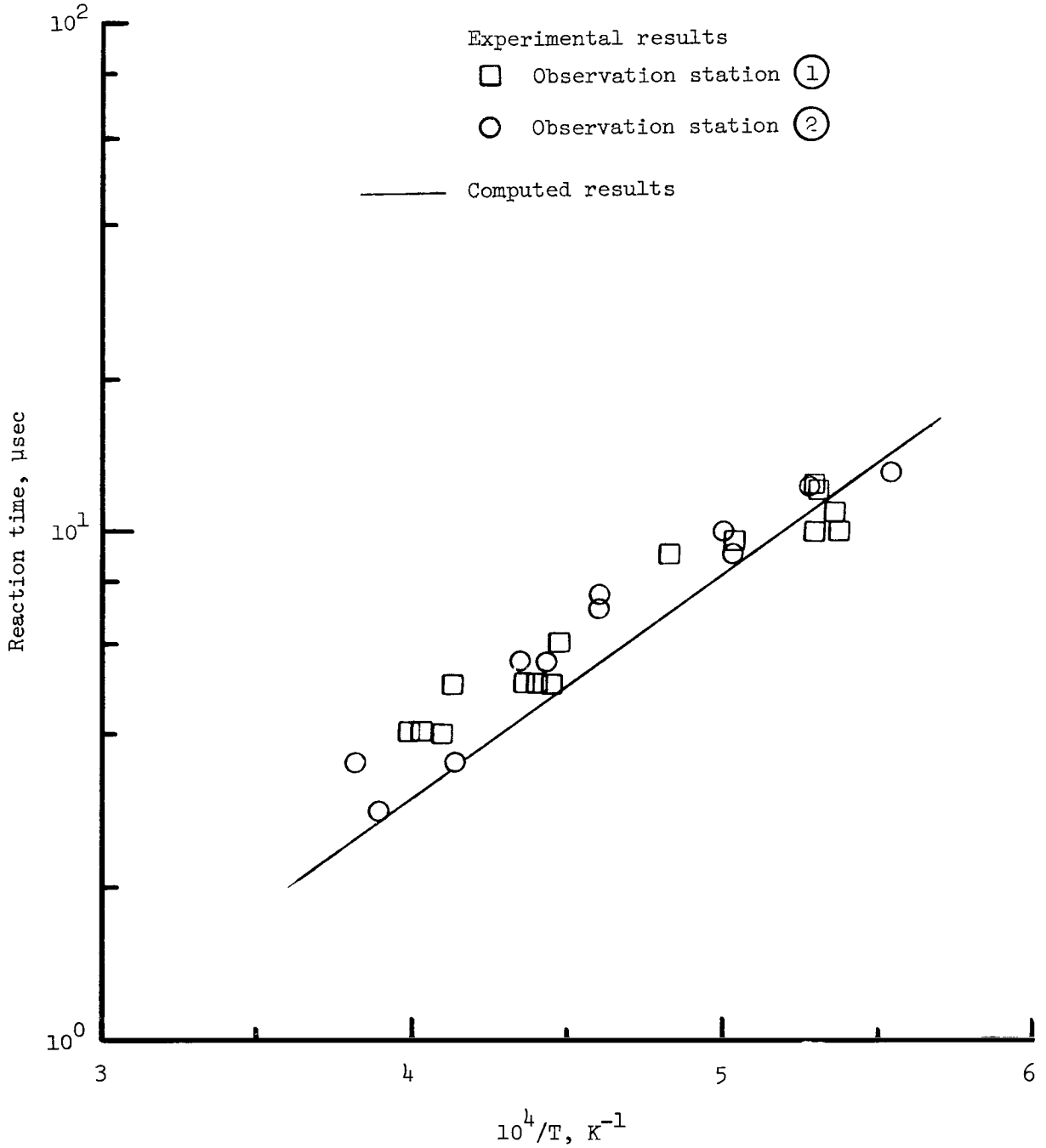

Figure 9.- Comparison of predicted and measured reaction times for stoichiometric combustion of propane.

NASA-Langley, 1977 L-11606

NATIONAL AERONAUTICS AND SPACE ADMINISTRATION
WASHINGTON, D.C. 20546

OFFICIAL BUSINESS
PENALTY FOR PRIVATE USE $300

SPECIAL FOURTH-CLASS RATE
BOOK

POSTAGE AND FEES PAID
NATIONAL AERONAUTICS AND
SPACE ADMINISTRATION
451

U.S.MAIL

POSTMASTER: If Undeliverable (Section 158 Postal Manual) Do Not Return

"The aeronautical and space activities of the United States shall be conducted so as to contribute . . . to the expansion of human knowledge of phenomena in the atmosphere and space. The Administration shall provide for the widest practicable and appropriate dissemination of information concerning its activities and the results thereof."

—NATIONAL AERONAUTICS AND SPACE ACT OF 1958

NASA SCIENTIFIC AND TECHNICAL PUBLICATIONS

TECHNICAL REPORTS: Scientific and technical information considered important, complete, and a lasting contribution to existing knowledge.

TECHNICAL NOTES: Information less broad in scope but nevertheless of importance as a contribution to existing knowledge.

TECHNICAL MEMORANDUMS: Information receiving limited distribution because of preliminary data, security classification, or other reasons. Also includes conference proceedings with either limited or unlimited distribution.

CONTRACTOR REPORTS: Scientific and technical information generated under a NASA contract or grant and considered an important contribution to existing knowledge.

TECHNICAL TRANSLATIONS: Information published in a foreign language considered to merit NASA distribution in English.

SPECIAL PUBLICATIONS: Information derived from or of value to NASA activities. Publications include final reports of major projects, monographs, data compilations, handbooks, sourcebooks, and special bibliographies.

TECHNOLOGY UTILIZATION PUBLICATIONS: Information on technology used by NASA that may be of particular interest in commercial and other non-aerospace applications. Publications include Tech Briefs, Technology Utilization Reports and Technology Surveys.

Details on the availability of these publications may be obtained from:

SCIENTIFIC AND TECHNICAL INFORMATION OFFICE

NATIONAL AERONAUTICS AND SPACE ADMINISTRATION

Washington, D.C. 20546